



# Seismic and gravity anomaly evidence of large-scale compressional deformation off SW Portugal

T.A. Cunha<sup>a,b,\*</sup>, A.B. Watts<sup>a</sup>, L.M. Pinheiro<sup>c</sup>, R. Myklebust<sup>d</sup>

<sup>a</sup> Department of Earth Sciences, University of Oxford, Parks Road, Oxford OX1 3PR, UK

<sup>b</sup> Instituto Don Luiz (IDL-LA), Campo Grande C8, 1749-016 Lisboa, Portugal

<sup>c</sup> Department of Geosciences and CESAM, University of Aveiro, Campus de Santiago, 3810-193 Aveiro, Portugal

<sup>d</sup> TGS-NOPEC Geophysical Company ASA, Hagaløkveien 13, N-1383 ASKER, Norway

## ARTICLE INFO

### Article history:

Received 20 March 2009

Received in revised form 11 January 2010

Accepted 31 January 2010

Available online 12 March 2010

Editor: R.D. van der Hilst

### Keywords:

Passive margin

SW Portugal

seismic reflection data

gravity anomalies

flexure

## ABSTRACT

Multi-channel seismic and gravity anomaly data have been used to determine the extent of compressional deformation along the SW Portugal rifted continental margin and place constraints on the long-term (>1 M.a.) strength of the lithosphere. The seismic sections suggest that the region of compressional deformation is broad (~100 km) and has been active since the Miocene. Integration with recently compiled high-resolution bathymetric data shows that the main thrust front is located along the base of the continental slope, between north of the Gorringe Bank and the Setúbal Canyon. Gravity data show that the thrust front is associated with a narrow isostatic anomaly 'high' of up to 70 mGal that is flanked on its NW edge by a broad 'low' of up to 20 mGal. This high-low 'couple' can be explained by compressional loading of extended continental lithosphere that increased its flexural strength (or equivalent elastic thickness,  $T_e$ ) since rifting. Based on combined 2-D backstripping and gravity modelling techniques we estimate a  $T_e$  of ~10 km during the main stretching episode, in the Late Jurassic (maybe earliest Cretaceous?), and of 35–50 km during the Miocene to Recent compression. The existence of a broad region of deformation off SW Portugal together with a strong lithosphere have implications for the rupture models of large earthquakes in the region, such as the 1755 Great Lisbon earthquake, particularly when accounting for a complex, multiple rupture in faults which cut through lithosphere of distinct nature and origin, as appears to be required by modellers to explain the historical observational data.

© 2010 Elsevier B.V. All rights reserved.

## 1. Introduction

The SW Portugal passive margin formed through a sequence of rifting events associated with the opening of the North Atlantic and the break-up of Iberia and North America during the Early Cretaceous (e.g. Wilson et al., 1989; Pinheiro et al., 1992, 1996; Alves et al., 2009). This was followed by a Mid-Miocene to Recent approximately NW–SE directed compression (Mauffret et al., 1989; Ribeiro et al., 1996), associated with the Africa–Eurasia plate convergence, the progressive closure of the Tethys oceanic basins and the westwards propagation of the Betic–Rif collision (Dewey et al., 1989; Maldonado et al., 1992; Rosenbaum et al., 2002). According to recently derived kinematic plate models based on space geodetic observations, the present-day convergence rate between NW Africa and Iberia is ~4.5–6 mm yr<sup>-1</sup>, with a NW–SE to WNW–ESE shortening direction (e.g. Sella et al., 2002; Calais et al., 2003; Fernandes et al., 2003 – red arrow in the inset of Fig. 1a); i.e. significantly tilted in relation to the predictions from previous kinematic plate solutions based on geological and geophysical

observations (Argus et al., 1989; DeMets et al., 1994 – model NUVEL-1A; black arrow in the inset of Fig. 1a).

The margin is presently located in the eastern segment of the Azores Gibraltar plate boundary (see inset in Fig. 1a). The region is commonly interpreted as a diffuse plate boundary, characterized by widespread seismicity and by a broad region of distributed compressive/transpressive deformation (~200–300 km between the Seine Abyssal Plain and the SW Portugal margin; Fig. 1a), which extends over old oceanic, continental and, possibly, transitional-type lithosphere (Grimison and Chen 1986; Sartori et al., 1994; Hayward et al., 1999; Buforn et al., 2004; Zitellini et al., 2004; Rovere et al., 2004). Historical records show that the active faults in this complex tectonic framework can generate very large earthquakes and destructive tsunamis, such as the 1st November 1755 event (estimated  $M = 8.5–8.7$ , Abe, 1979;  $M_w = 8.7 \pm 0.4$ , Johnston, 1996;  $M_w = 8.5 \pm 0.3$ , Solares and Arroyo, 2004). The largest instrumental earthquake recorded in the area was the 28th of February 1969 ( $M_w = 7.8$ ; Fukao, 1973), localized in the Horseshoe abyssal plain (Fig. 1a) with a thrust fault mechanism.

The source of the large 1755 earthquake has been generally attributed to rupture within old, strong oceanic lithosphere in the Horseshoe Abyssal Plain or the Gorringe Bank (Grimison and Chen, 1986; Johnston, 1996; Stich et al., 2007). Baptista et al. (1998, 2003),

\* Corresponding author. Current address: Unidade de Geologia Marinha - LNEG, Estrada da Portela, Zambujal-Alfragide, 2720-866 Amadora, Portugal. Tel.: +351 214705541; fax: +351 214719018.

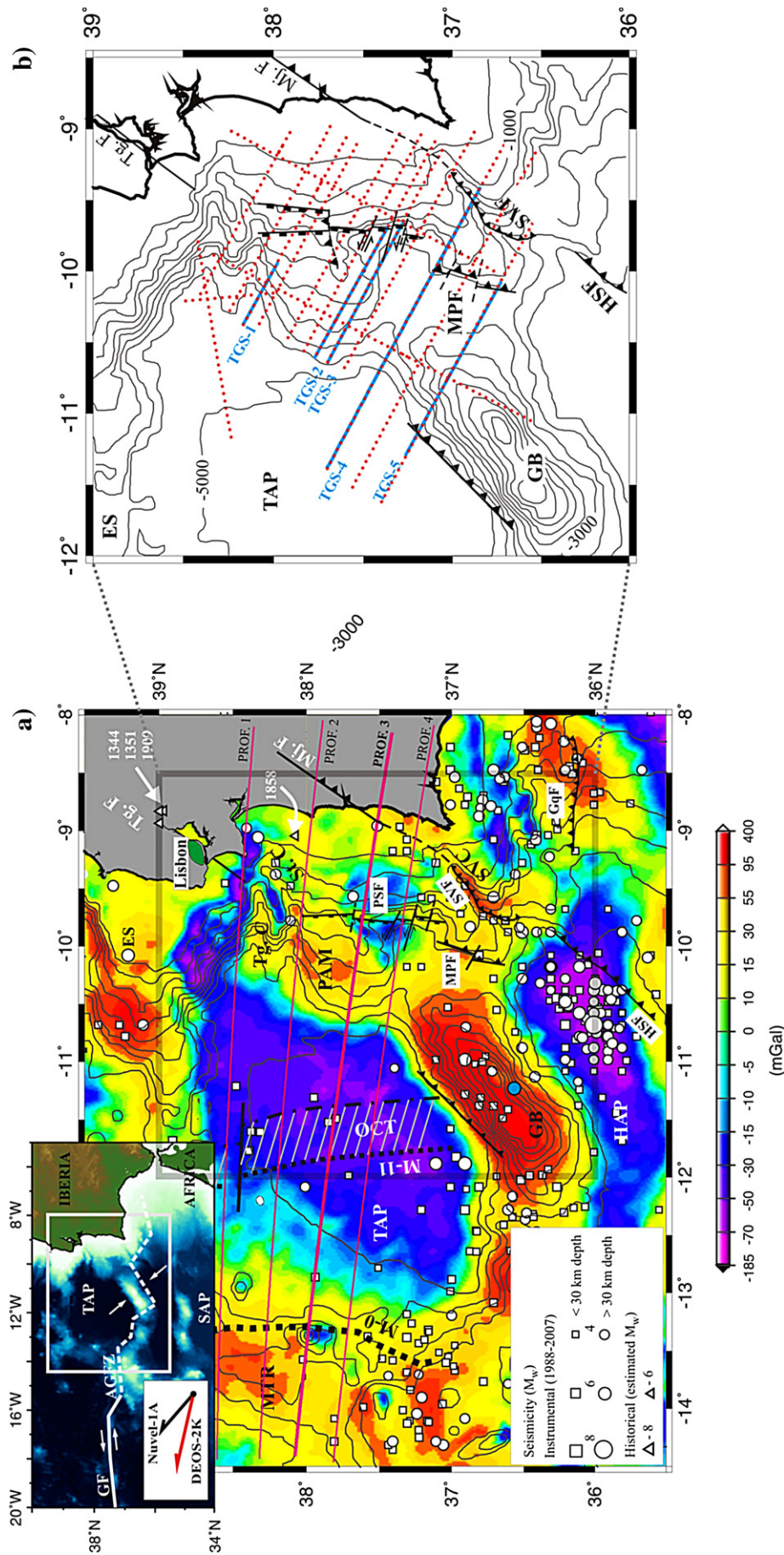


**Fig. 1.** a) Sediment corrected Airy isostatic anomaly off SW Portugal with 500 m bathymetric contours. Pink lines show the location of the 4 gravity modelled profiles. The modelling results along Profile 3 (thick line) will be discussed in detail (Figs. 5 and 6). Also depicted is the instrumental (http://www.iris.edu) and historical (Botges et al., 2001, and references therein) seismicity of the region; the Ocean-Continent Transition (OCT), defined between magnetic anomaly M-11 and the limit of continental-type crust (Pinheiro et al., 1992, 1996); DSDP site 120, leg 13 (blue dot); and the main structural elements previously mapped in the region (Zitellini et al., 2001; Terrinha et al., 2003; Gràcia et al., 2003). The inset in the top left corner shows the location of the area with the approximate position of the Africa-Eurasia plate boundary (the Azores Gibraltar Fracture Zone, AGFZ; Ribeiro et al., 1996). The arrows in the bottom left corner show the predicted motion of Africa in relation to Eurasia (at the centre of the Gulf of Cadiz, GC) according to GPS-derived kinematic plate models (e.g. Fernandes et al., 2003; red arrow) and the NUVEL-1A global kinematic plate model of DeMets et al. (1994; black arrow). b) Bathymetry (500 m contours), previously mapped main structures and location of the TGS-Nopec multi-channel seismic lines utilized in this study (dotted red lines). The lines highlighted in blue are depicted in Fig. 2 (Line TGS-3); Fig. 3 (Line TGS-4), and in the Supplementary Material Figs. SM1 to SM5 (fully interpreted colour versions of lines TGS-1 to 5, respectively). Acronyms are as follows: ES, Estremadura Spur; GB, Gorringe Bank; GC, Gulf of Cadiz; GF, Gloria Fault; GqF, Guadalquivir Fault; HAP, Horseshoe Abyssal Plain; MPF, Marquês de Pombal Fault; MTR, Madeira-Tore Rise; Mj.F, Messejana Fault; PAM, Príncipes d’Avis Mountains; PSF, Pereira de Souza Fault; SAP, Seine Abyssal Plain; St.C, the Setúbal Canyon; SVC-F, Saint Vincent Canyon-Fault; TAP, Tagus Abyssal Plain; Tg-C-F, Tagus Canyon-Fault.

however, based on the tsunami hydrodynamic modelling results and the isoseismal distribution in the Iberia Peninsula, constrained the source for the 1755 Lisbon earthquake and tsunami in the proximity of the SW Portugal continental shelf, possibly involving co-seismic rupture in several fault segments. All the proposed models require a thick brittle lithosphere, involving also the upper mantle, to accommodate the energy release along an estimated 200–300 km long compound fault (Johnston, 1996; Ribeiro et al., 2006; Stich et al., 2007). The brittle properties of the upper mantle in this area is reflected in the occurrence of earthquakes at sub-crustal depths (>30 km), recorded both in old oceanic and continental lithosphere, as depicted in Fig. 1a.

The SW Portugal margin is also characterized by large-amplitude and short wavelength Airy isostatic gravity anomalies, the most prominent of which is a positive–negative anomaly “couple” which extends from the Gorringe Bank, along the lower part of the slope and rise, to the Setúbal Canyon (Fig. 1a). Such a couple is commonly observed over fold and thrust belts and their associated foreland basins (e.g. Karner and Watts, 1983) where it has been attributed to orogenic loading and flexure. Indeed, Hayward et al. (1999) have shown that the positive–negative anomalies centred at latitude 37°N and longitude 11.5°W can be explained by a model in which the NW flank of the Gorringe Bank flexurally loaded old oceanic crust of the southern Tagus Abyssal Plain (TAP).

Despite the recent acquisition of a number of large, high quality marine geophysical datasets, there is still much debate on the distribution of compressional deformation and its significance for the structure, evolution and seismicity of the margin (Ribeiro et al., 1996; Terrinha et al., 2003; Zitellini et al., 2004; Stich et al., 2007). In this paper, we use new, high quality Multi-Channel Seismic (MCS) profile data and recently compiled high-resolution bathymetry (the SWIM compilation; Diez et al., 2005), together with sediment thickness data (Cunha, 2008) and Process Oriented Gravity Modeling (POGM) techniques (e.g. Stewart et al., 2000), to constrain the spatial extent of compressional deformation at the margin and examine its implications for the crustal structure, the long-term strength of stretched continental lithosphere, and the rupture mechanisms of large earthquakes.

## 2. Structural framework of the SW Portugal margin

The SW Portugal margin is characterized by a series of extensional grabens, half-grabens, and horsts, delimited by predominately N–S and ENE–WSW trending faults (Wilson et al., 1989; Pinheiro et al., 1996; Alves et al., 2009) inherited from the late stages of Variscan deformation (late Carboniferous–Permian; Arthaud and Matte, 1977; Ribeiro et al., 1990). According to Alves et al. (2009), most of the fault-driven subsidence in the continental slope area occurred in the Late Jurassic (possibly earliest Cretaceous?). This was followed by the development of a relatively wide Ocean–Continent Transition (50–110 km wide) between the continental rise and magnetic anomaly M-11 (Fig. 1a), and continental break-up in late Valanginian/early Hauterivian (Pinheiro et al., 1992, 1996). From the Mid-Miocene onwards, some major rift-related structures have been reactivated in compression/transpression (Mauffret et al., 1989; Terrinha et al., 2003; Zitellini et al., 2004; Alves et al., 2009). This is particularly noticeable in the distal margin (i.e. along the continental slope and rise; Alves et al., 2009), where the thrusting and folding are, in places, associated with the formation of prominent bathymetric features (e.g. the Marquês de Pombal and Principes d'Avis mountain; Zitellini et al., 2004).

Recently acquired swath-bathymetry, side-scan sonar imagery and seismic reflection profiles (Zitellini et al., 2001; Gràcia et al., 2003; Terrinha et al., 2003) also revealed the existence of complex channel–levee systems, mass wasting deposits and slump scars associated with seafloor slope ruptures. The data confirm the recent activity of several fault systems (Gràcia et al., 2003; Terrinha et al.,

2003; Zitellini et al., 2004; Vizcaino et al., 2006), one of which is the Marquês de Pombal Fault (MPF), a deep-rooted landward-dipping thrust associated with a 55 km long and almost 1000 m high escarpment (Fig. 1). This fault has been interpreted as the probable source of the 1755 Lisbon Earthquake (Zitellini et al., 2001) and its location is consistent with previous epicentral estimates based on tsunami travel-time and amplitude data (Baptista et al., 1998, 2003). However, the area of rupture appears insufficient to produce an event the size of the Lisbon earthquake (Johnston, 1996; Stich et al., 2007). This suggests a possible multiple rupture on the MPF and other active faults in the region (e.g. Zitellini et al., 2001; Terrinha et al., 2003; Baptista et al., 2003).

In this paper, we present examples of a dense grid of high quality, previously unpublished, seismic reflection profiles acquired by TGS-Nopec in 2000/01 between the Tagus and St. Vincent canyons (the subset of seismic lines used in this work is depicted in Fig. 1b by the dotted red lines). The new data considerably improves the previous coverage over the Principes d'Avis Mountains (PAM) and the southeastern Tagus Abyssal Plain, and allows a much better constrained interpretation of the shallow and deep structure of the margin in these areas. Figs. 2 and 3 show a structural interpretation of two of these seismic lines (lines TGS-3 and TGS-4 in Fig. 1b). Also depicted is the Mid-Miocene angular unconformity (dotted line), which marks the onset of compressional deformation in the SW Portugal rifted margin (Mauffret et al., 1989). The original and fully interpreted colour versions of 5 TGS-Nopec seismic lines used in this work are shown in Supplementary Material – Figs. SM1 to SM5 (EPSL Supplementary Material<sup>1</sup>; see Fig. 1b for location).

In the PAM region, Line TGS-3 (Fig. 2) shows a thick sedimentary basin (2–3 s TWT), the Principes d'Avis Basin, which has been uplifted and compressional deformed. The major structures observed here comprise 2 asymmetric folds, with a NW transport direction, delimited by reverse faults (the 2 westernmost being antithetic to the Pereira de Sousa normal fault, PSF). These thrusts are here designated as the Principes d'Avis Thrusts (T1, T2 and T3, in Figs. 2, 4 and SM2–3). Further to the west, a localized pop-up structure controlled by an ESE dipping thrust disrupts the Mid-Miocene to Recent sediments and the seafloor, which suggests that it has been recently active (Pliocene–Quaternary). This thrust strikes NNE–SSW along the base of the continental slope between north of the Gorringe Bank and the Setúbal canyon (Fig. 4) and we believe it represents the westernmost major front of the compressional deformation. Terrinha et al. (2003) inferred a thrust fault at an approximate location, but could not constrain its orientation or spatial extent. In the high-resolution bathymetry 3-D block diagram presented in Supplementary Material Fig. SM6, the trace of the TAP-thrust can be followed for ~50 km, associated with a number of slope failures.

A feature of the mapped thrust faults is their lack of continuity along-strike the SW Portugal margin (blue lines in Fig. 4). For example, the main TAP-thrust in the PAM region does not appear to extend into the thrusts bounding the Gorringe Bank in the south (see Supplementary Material; Fig. SM5) or the Setúbal and Tagus canyons in the north (Fig. SM1). Moreover, the PAM are a distinct bathymetric region that is bounded by across-strike topographic depressions in the margin. These observations suggest that the margin is highly segmented as regards its along-strike structure, possibly associated with the activity of NW–SE left-lateral wrench faults or transfer zones (dashed blue lines in Fig. 4).

<sup>1</sup> EPSL Supplementary Material XXXX; Includes the colour versions of 5 original and interpreted seismic reflection profiles from the TGS-Nopec 2000/01 speculative survey (Figs. SM1 to SM5), a 3-D block diagram of a high-resolution bathymetric dataset (the SWIM bathymetry; Fig. SM6), the POGM results along 4 profiles (Fig. SM7), and the colour versions of Figs. 5 and 6 of the paper.

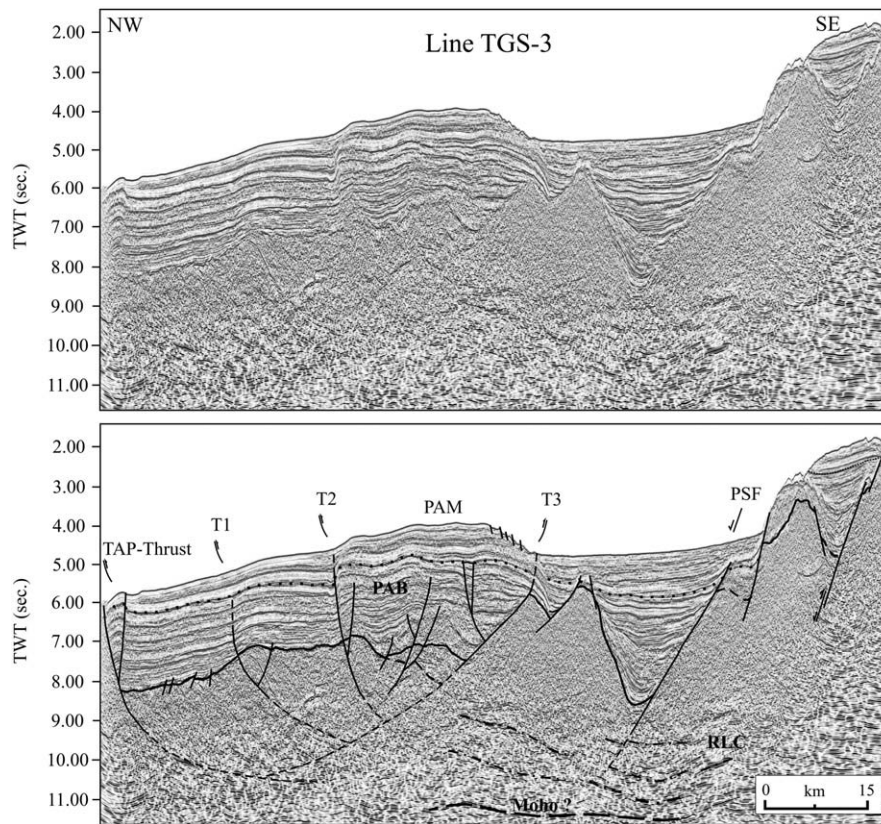


**Fig. 2.** Main structural elements and interpreted basement and Moho along Line TGS-3 (see Figs. 1b and 4 for location). The position of the Mid-Miocene unconformity is highlighted by the dotted line. The TAP-Thrust is here interpreted as the westernmost major thrust front of the Mid-Miocene to Recent compressional deformation (see text). The Príncipe d'Avis Thrusts T1, T2 and T3 were also identified in this study and show lateral continuity in the region of the PAM (Fig. 4). PAB stands for Príncipe d'Avis Basin and RLC indicates the reflective lower crust. Other acronyms are as in Fig. 1. Vertical exaggeration of the seismic section is  $\sim 8\times$ . A structural and stratigraphic interpretation of this and 4 other MCS lines is presented in colour in Supplementary Material Figs. SM1–SM5; where we also describe the main steps of the seismic processing sequence.

Line TGS-4 (Fig. 3) shows the Mid-Miocene to Recent compressional deformation being accommodated over a broad area between the St. Vincent Canyon and the eastern TAP (see Fig. 4 for location). Near the base of the continental slope, two well-defined rotated continental blocks are observed (blocks B2 and B3). These are followed to the west by what is interpreted as an extremely thin crust underlain by a strong E-dipping reflector beneath blocks B2, B1 and R. This reflector, interpreted here as the Moho, is observed at  $\sim 11$  s TWT in the region of block B2 and shallows to  $\sim 9$  s TWT near the western end of the seismic line, where it directly underlies post-rift sediments. This location corresponds to the eastern limit of the 'transitional crust' defined by Pinheiro et al. (1996; Figs. 1 and 4), which is interpreted as serpentinized peridotite at the Ocean–Continent Transition (OCT). Block R can either be a very thin rotated continental block or a small serpentinized mound, or ridge.

The TGS-Nowec seismic data interpreted in this study allow us to better constrain the direction and extent of the main compressional structures in the distal SW Portugal margin, particularly in the western and northern PAM and the southeastern TAP (dark grey shaded area in Fig. 4). Together with previously published data (Terrinha et al., 2003; Zitellini et al., 2004), we infer an approximately 100 km wide region where most of the Mid-Miocene to Recent compressional deformation is being accommodated between north of the Goringe Bank and the Setúbal Peninsula (light and dark grey shaded areas in Fig. 4). The region is delimited by the TAP-thrust, which follows the base of the continental slope, and the Pereira de Sousa Fault, to the east, which is a normal fault continuous for more than 60 km (Terrinha et al., 2003) that marks the easternmost limit of the main compressional structures (Figs. 2 and 4).

### 3. Results from process oriented gravity modelling

The free-air gravity "edge-effect" anomaly at a passive continental margin can be considered as the sum of all the processes that have affected it through time (Watts, 1988). These include rifting and sedimentation. By applying POGM techniques it is possible to quantify the effects of these extensional-related processes (e.g. Stewart et al., 2000) and to isolate the contributions from other processes, such as those associated with compressional deformation.

The first step in POGM is to backstrip the sediments in order to recover the tectonic subsidence of a margin for different assumptions of the elastic thickness,  $T_e$  (sed), which is a proxy for the long-term flexural strength of the lithosphere (Watts, 1988). Then, the backstrip is used to restore the crustal structure of the margin at the time of rifting, assuming either no strength (i.e.  $T_e$  (rift) = 0) or finite strength (i.e.  $T_e$  (rift)  $\neq 0$ ; Kooi et al., 1992) during rifting. We use here the formulation of Watts and Stewart (1998), which allows the Moho to be determined directly from the tectonic subsidence (TS) for a given  $T_e$  (rift) and  $Z_{neck}$ , a parameter that defines the depth of stress maxima and, hence, necking depth (Kooi et al., 1992). The final step is to calculate the gravity anomaly due to rifting and sediment loading and to compare their sum to the observed free-air gravity anomaly in order to constrain  $T_e$  (sed),  $T_e$  (rift) and  $Z_{neck}$ . We note that with a 31 km thick, pre-stretched crust, and densities of 1030, 2780 and 3300 kg m<sup>-3</sup> for the water, crust and mantle, respectively, a  $Z_{neck}$  of 7.4 km corresponds to the Airy case (i.e.  $T_e$  (rift) = 0).

Fig. 5 shows the results of POGM along a WNW–ESE transect that extends from onshore SW Portugal, across the PAM and the Tagus

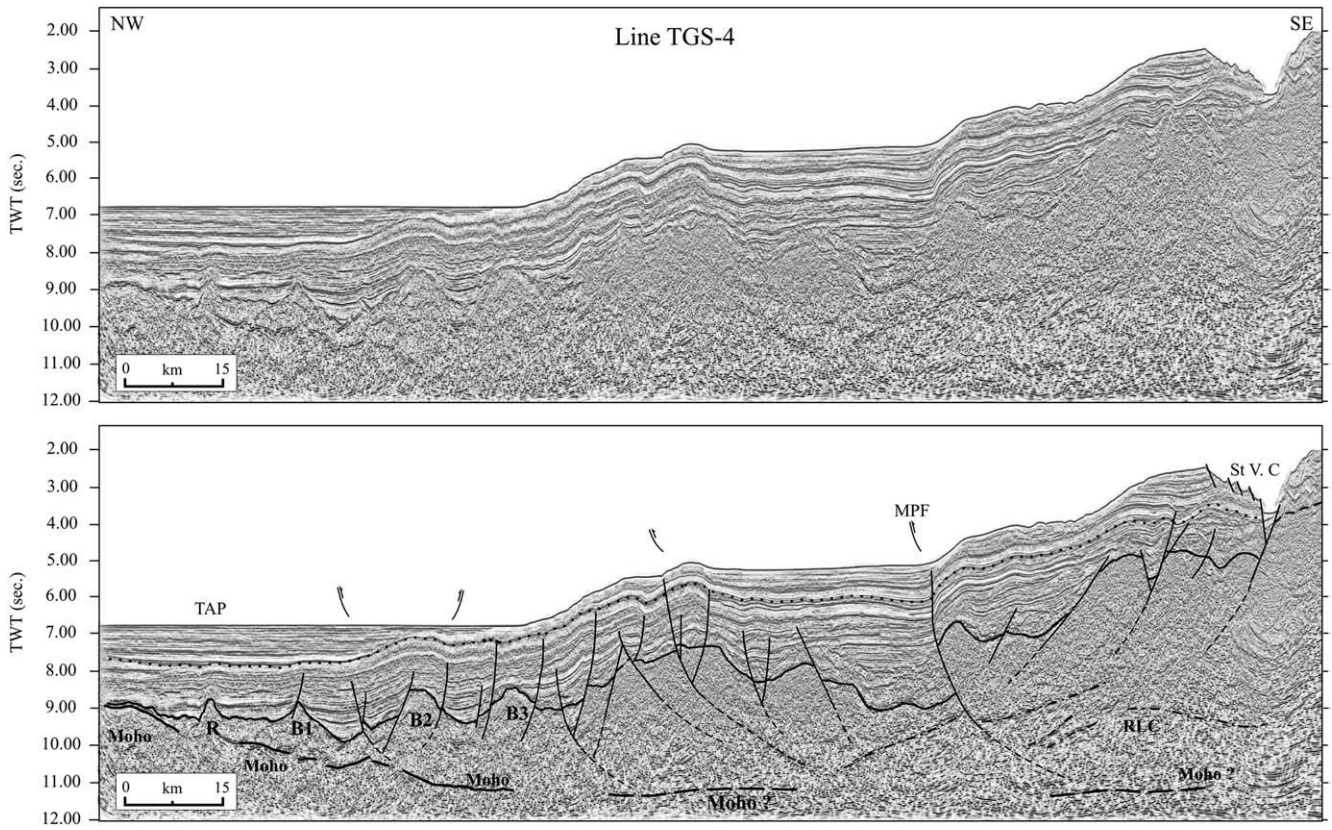


**Fig. 3.** Main structural elements and interpreted basement and Moho along Line TGS-4 (see Figs. 1b and 4 for location). The position of the Mid-Miocene unconformity is highlighted by the dotted line. The nature of the basement blocks R, B1, B2 and B3 is discussed in the text and RLC indicates the reflective lower crust. Other acronyms are as in Fig. 1. Vertical exaggeration of the seismic section is ~8×. A structural and stratigraphic interpretation of this line is presented in colour in Supplementary Material; Fig. SM4.

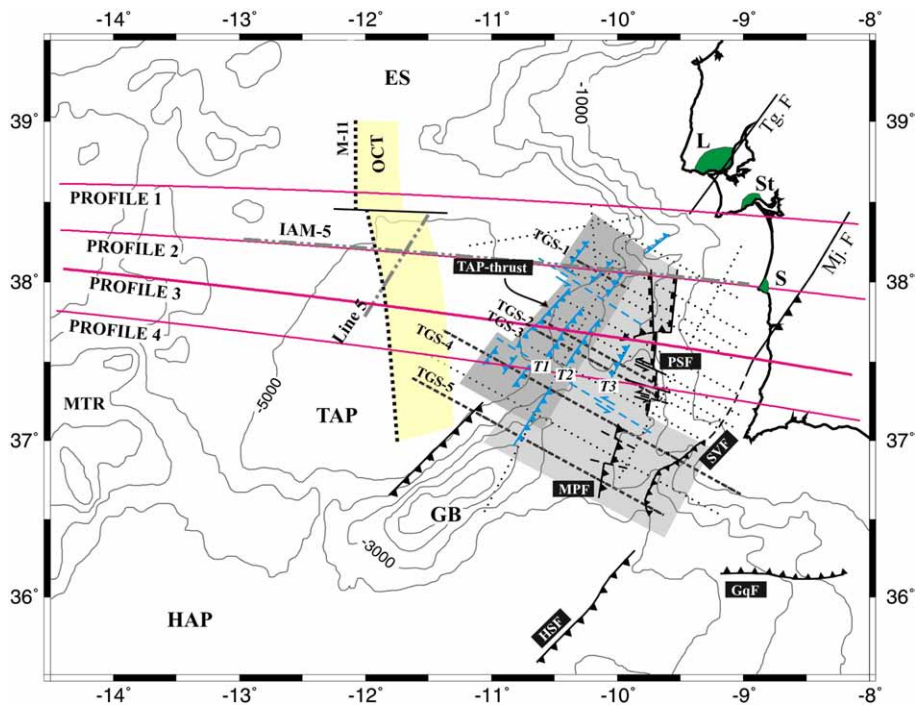


**Fig. 4.** Simplified bathymetric map (1000 m contours) showing the main structural elements in the distal SW Portugal margin. The thrust faults in blue have been mapped in this study (see text for the nomenclature of the structures). The dark grey shaded area highlights the region where the seismic data interpreted in this study significantly improved the mapping of the main compressional structures. Together with the light grey shaded area it defines the zone where most of the Mid-Miocene to Recent compressional deformation is accommodated. The dotted lines represent the interpreted TGS-Nowepc seismic profiles, where the thick dashed ones are depicted in Fig. 2 (Line TGS-3), Fig. 3 (Line TGS-4), and in the Supplementary Material Figs. SM1 to SM5. Also shown is the location of the gravity modelled profiles (pink lines) and of the wide-angle seismic data used to constrain the results of the gravity modelling (thick dotted-dashed grey lines; see Fig. 6). Acronyms are as in Fig. 1. Green areas are cities along the Portuguese coast, namely: Lisbon (L), Setúbal (St) and Sines (S).

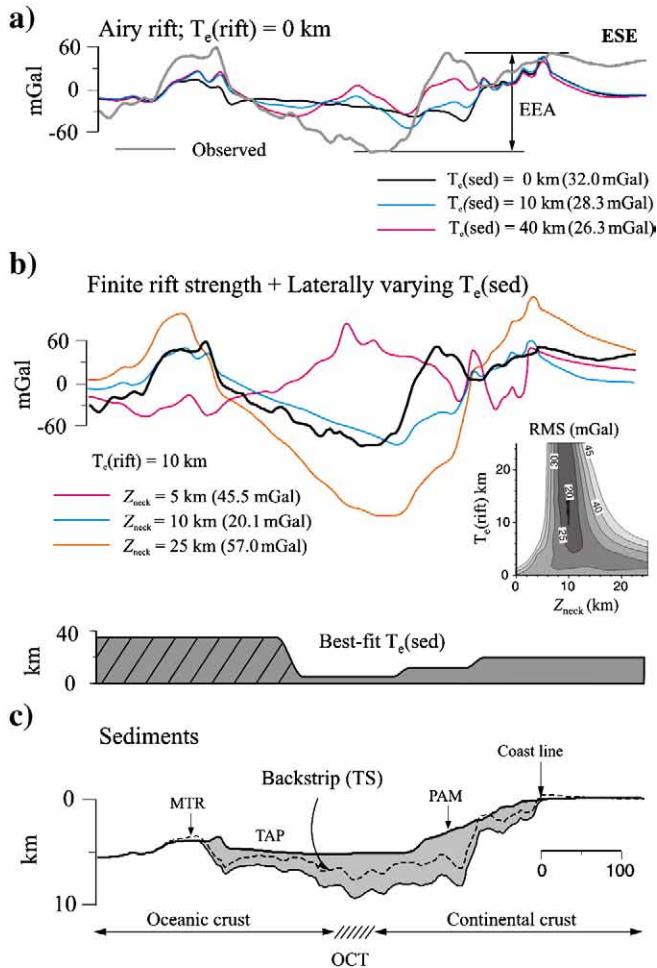


**Fig. 5.** Results from Process Oriented Gravity Modelling (POGM) along a WNW-ESE transect extending between onshore Portugal and the Madeira-Tore Rise (Profile 3 in Figs. 1a and 4). a) Comparison between observed (satellite-derived, Sandwell and Smith, 1997) and calculated (POGM) free-air gravity anomalies assuming an Airy model of rifting (i.e.  $T_e(\text{rift}) = 0$  km). The RMS difference is indicated within brackets for the different  $T_e(\text{sed})$  scenarios. EEA is the “edge-effect” free-air gravity anomaly. b) Comparison between observed and calculated free-air gravity anomalies assuming finite rift strength and a laterally varying  $T_e(\text{sed})$  – grey bar shown below, where the hatched area indicates the regions where the sediment thickness grid, and thus the results from POGM, are less well constrained. The ‘best fit’ model is obtained with a  $T_e(\text{rift}) = 10$  km and  $Z_{\text{neck}} = 10$  km (see RMS inset graphic). c) Sediments and backstrip surface for the best fit  $T_e(\text{sed})$ . The basement depths were extracted from a recently compiled dataset for the whole of the West Iberia Margin (Cunha, 2008). Acronyms are as in Fig. 1. A colour version of Fig. 5 is presented in Supplementary Material (Fig. SM8).

Abyssal Plain, to the Madeira-Tore Rise (Profile 3 in Figs. 1a and 4). The figure shows that:

- 1 - There are large differences along the profile (Root Mean Square difference,  $\text{RMS} = 32.0$  mGal) between the observed gravity anomaly and the calculated anomaly based on an Airy isostatic model (i.e.  $T_e(\text{sed}) = T_e(\text{rift}) = 0$  km; Fig. 5a).
- 2 - The RMS difference is reduced by assuming  $T_e(\text{sed}) > 0$  and  $T_e(\text{rift}) = 0$  km (Fig. 5a) and/or  $T_e(\text{sed}) = 0$ ,  $T_e(\text{rift}) > 0$  km and  $Z_{\text{neck}} > 7.4$  km. The best overall fit is for a spatially varying  $T_e(\text{sed})$ ,  $T_e(\text{rift}) = 10$  km and  $Z_{\text{neck}} = 10$  km ( $\text{RMS} = 20.1$  mGal; Fig. 5b).
- 3 - Despite the wide range of rifting and sediment loading parameters tested (see RMS graphic in Fig. 5b), no rifting and sediment loading model is able to explain the high-low free-air gravity anomaly couple over the continental slope and rise.

We believe that the most plausible explanation of the couple is that it is caused by Mid-Miocene to Recent compressional deforma-

tion of the margin. Seismic reflection profile data (Fig. 2 and Supplementary Material Figs. SM2–3) indicate that the PAM crust has been shortened and thickened along a number of deeply penetrating thrusts. We have therefore used a POGM-type approach to model the flexure and gravity anomaly that may have resulted from thrust loading.

The procedure involves 4 main steps (see Fig. 6). First, we use the best fitting rifting and sediment loading model to compute the gravity anomaly due to rifting and sediment loading and isolate the contribution of thrust loading and flexure. Second, we use the positive

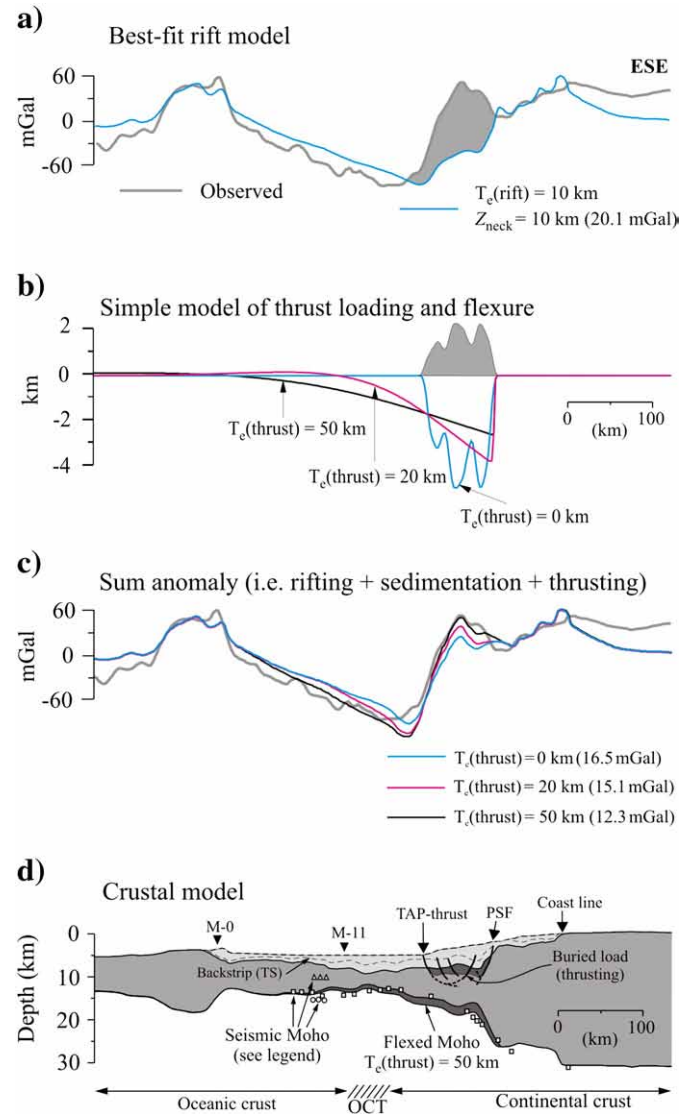


**Fig. 6.** Modelling procedure used to recover the size and gravity signal of the thrust loads and final gravity and crustal models. a) Observed free-air gravity anomaly and the best fit gravity model obtained from the contributions of rift and sediment loading (Fig. 5b). We attribute the isostatic gravity anomaly high over the lower continental slope (shaded area) to the existence of buried, thrust loading (see text). b) Equivalent load to the shaded area in (a) and corresponding flexure for a  $T_e(\text{thrust})$  of 0, 20 and 50 km. c) Comparison between observed and calculated gravity anomalies, where the calculated is the sum of the contributions from rifting, sedimentation and thrusting. d) Crustal structure based on the best fit model in (c); i.e. for a  $T_e(\text{thrust}) = 50$  km. Thrusts in the region of the PAM are a schematic representation of the structures identified in the TGS multi-channel seismic lines (Figs. 2 and SM3–4). Seismic constraints on the Moho depth are as follows (see Fig. 4 for location): white filled squares, projected from Line IAM-5 (Afilhado et al., 2008); white filled triangles and circles correspond to the top and base of the high velocity layer in Line 5 (Pinheiro et al., 1992), respectively. Acronyms are as in Fig. 1. A colour version of Fig. 6 is presented in Supplementary Material (Fig. SM9).

part of this resulting anomaly (shaded area in Fig. 6a) to constrain the geometry of the thrust load and then calculate the flexure and gravity anomaly for different assumed values of  $T_e$  (thrust) at the time of loading (Fig. 6b). We use a discontinuous, or broken plate model to calculate the flexure, similar to that used by Karner and Watts (1983) and Watts and Talwani (1974) in other compressional settings, and placed the plate break at the approximate location of the Pereira de Sousa normal fault. Third, we compute the combined gravity effect of the load and flexure, which we dub here the ‘thrusting anomaly’. Finally, the thrusting anomaly is added to the rifting and sediment loading anomalies and the sum compared to the observed gravity anomaly (Fig. 6c).

Fig. 6c shows that there is good agreement between the observed gravity anomaly and the anomaly calculated by summing the effects of rifting, sediment loading and thrusting. The best fit is for a  $T_e$  (thrust) = 50 km (RMS = 12.3 mGal). This model explains the main details of the observed gravity anomaly, particularly the ‘twin peaks’ of the shelf/slope high and the flanking low. Furthermore, Fig. 6d shows that the flexed Moho (i.e. the sum of the Moho restored from sediment backstripping and the flexure due to sediment and thrust loading) implied by the best fit model is in excellent agreement with the seismic Moho constrained by wide-angle data (dotted-dashed grey lines in Fig. 4) along Line IAM-5 (Afilhado et al., 2008) and Line 5 (Pinheiro et al., 1992, 1996).

The results from POGM along 4 ENE–WSW profiles in the SW Portugal margin (pink lines in Figs. 1 and 4) are summarized in Fig. 7, in terms of the isostatic anomalies power spectra at different stages of the modelling. The corresponding gravity and crustal models are depicted in Supplementary Material (Fig. SM7), and show a consistent  $T_e$  (sed) structure (decreasing from the continental shelf to the slope/rise and transitional domain),  $T_e$  (rift) and  $Z_{neck}$  along the margin. We observe that in profiles 2, 3 and 4, the higher amplitude Airy isostatic anomalies (solid grey lines in Fig. 7) are only efficiently reduced when

the effects of thrust loading are taken into account (thin black lines). Furthermore, in profiles 3 and 4, where the results are most sensitive to  $T_e$  (thrust), a  $T_e$  (thrust) = 50 km is recovered. Along Profile 11, the observed free-air anomalies can be explained from the rifting and sediment loading alone. This suggests that, offshore, most of the compressional deformation occurs to the south of Tagus Canyon.

#### 4. Discussion and conclusions

The results of this work have implications for the spatial distribution of compressional deformation off SW Portugal, the seismic hazard of the region, and the long-term strength of stretched continental lithosphere.

The seismic data suggest that the Mid-Miocene to Recent compressional deformation is being accommodated over an arcuate, ~100 km wide (delimited by the PSF and the TAP-thrust) and 150 km long, region between the Gorringe Bank and the Setúbal Peninsula (Fig. 4). Together with the recently compiled high-resolution SWIM bathymetric dataset (Supplementary Material, Fig. SM6), the data constrains the location of the westernmost major thrust front, the TAP-thrust, at the base of the continental slope. The TAP-thrust may continue to the SW and link with the thrust at the base of the Gorringe Bank, as suggested by Ribeiro et al. (1996). However, we interpret that the PAM region is separated from the Gorringe Bank by a NW–SE transfer zone that follows a broad topographic depression and laterally offsets the NNE-trending main thrust front to the north from the similar trending MPF thrust to the south (Fig. 4).

Such a tectonic framework has important implications when estimating the rupture areas of large earthquakes and associated tsunamis in the region (e.g. Baptista et al., 1998; Zitellini et al., 2001; Gutscher et al., 2002; Terrinha et al., 2003; Stich et al., 2007). We speculate, for example, that a compound, multiple rupture may involve several major NNE–SSW to NE–SW trending fault systems, including the TAP-thrust (~50 km), the MPF (~60 km length; Zitellini et al., 2001; Terrinha et al., 2003; Baptista et al., 2003), and possibly also the Horseshoe Fault (~120 km; Gràcia et al., 2003; Zitellini et al., 2004; Ribeiro et al., 2006; Stich et al., 2007). Together, these three fault segments extend for approximately 230 km, which is within the rupture length estimated by Johnston (1996; 180–280 km) needed to generate a  $M_w = 8.7$ , “1755-like” major earthquake in the SW Portuguese margin, assuming a large stress drop (10–14 m displacement, respectively) associated with an old, strong oceanic lithosphere (up to 50 km thickness strong brittle layer; Grimison and Chen, 1986; Johnston, 1996; Stich et al., 2007). The implications of such source characteristics for the models which involve rupture of the stretched continental and/or transitional lithosphere, as proposed here and by a number of authors before (e.g. Zitellini et al., 2001; Terrinha et al., 2003; Baptista et al., 2003; Ribeiro et al., 2006; Stich et al., 2007) remain, however, a matter of debate.

The seismic and gravity anomaly data show that the deformed region is associated with large-amplitude isostatic gravity anomalies. The anomalies cannot be explained by crustal thinning at the time of rifting or post-rift sediment loading of a finite strength lithosphere. Rather, they require the addition of intra-crustal, thrust loads in order to fully explain them. Tests using POGM show that  $T_e$  (rift)  $\ll$   $T_e$  (thrust). Since most extensional deformation took place during the Late Jurassic–Early Cretaceous and the thrust loads were not emplaced until the Mid-Miocene to Recent, these results suggest that the strength of the thinned, extended lithosphere increases with age since rifting. This is consistent with the predictions of Burov and Poliakov (2001) based on dynamical models that weakened, rifted, continental lithosphere might regain its strength following rifting, and with the  $T_e$ 's compiled from a number of rift margins for a wide range of loading ages (where the age refers to elapsed time since rifting; Close et al., 2009). Rodger et al. (2006) have also inferred a significant strengthening of the lithosphere supporting the Amazon

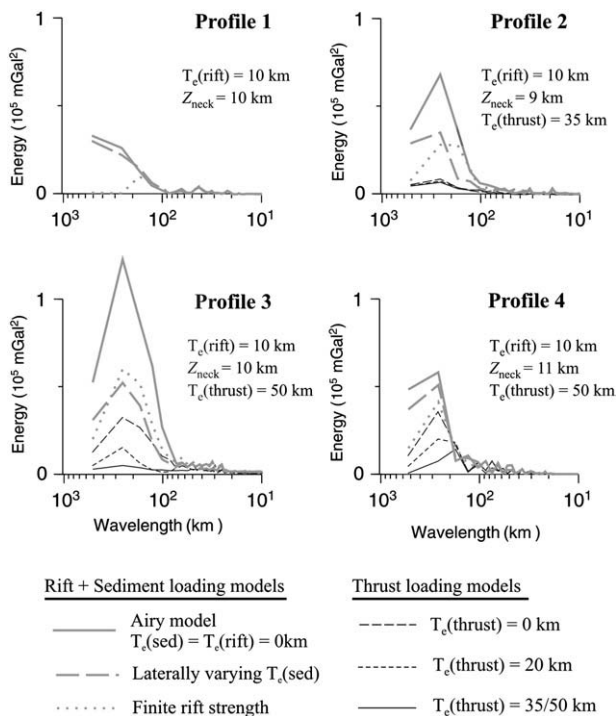


**Fig. 7.** Power spectra of the isostatic anomalies calculated at different stages of the gravity modelling in Profiles 1 to 4 (see Figs. 1a and 4 for location). For each profile, the  $T_e$  (rift),  $Z_{neck}$  and  $T_e$  (thrust) of the best fit gravity model are indicated. The corresponding gravity and crustal models, as well as the best fit  $T_e$  (sed), are shown in Supplementary Material (Fig. SM7). Note the importance of the thrust loading and the model sensitivity to  $T_e$  (thrust) in Profiles 3 and 4.

Fan, in the northern Brazil rifted margin, which is underlain by highly stretched continental crust that abuts unusually thin oceanic crust.

As verified by Burov and Poliakov (2001) from yield strength envelope considerations, the increase in the strength of stretched continental lithosphere during post-rift times is caused by the replacement of weak lower crust by mantle/asthenosphere material, which rapidly cools and, eventually, becomes mechanically coupled with the thinned crust. Burov and Diament (1996) referred to this coupled state as an “oceanic” mode of the continental lithosphere strength profile. In such settings, the lithosphere effective elastic thickness ( $T_e$ ) becomes comparable with the seismogenic layer thickness ( $T_s$ ), despite the differences in their meaning and time-scales;  $T_s$  reflects the stress level on historical time-scales in the uppermost brittle layer of the lithosphere (see Watts and Burov, 2003 for discussion).

The strengthening of the lithosphere has implications for those rifted margins, such as SW Portugal, that have been subject to compressional deformation late in their history. In particular, an increasing strength has implications for the detachment surface that may link different thrust fault systems in depth, as previously suggested by Zitellini et al. (2001) and Terrinha et al. (2003) and, in fact, imaged on the hanging-wall of the MPF (Zitellini et al., 2001). A strong underthrusting lithosphere would be expected to be associated with a broader, shallower detachment than would a weak one. Moreover, a strong, coupled lithosphere justifies the use of the scaling models proposed by Johnston (1996), and later by Stich et al. (2007), when estimating the length of a rupture surface over both stretched continental and old oceanic lithosphere for a large, “1755-like” earthquake and tsunami in the SW Portugal region.

## Acknowledgments

The authors thank TGS-Nopec and DPEP, Portugal (T. Abecassis) for access to MCS data. This work was supported by the Fundação para a Ciência e Tecnologia, under the scholarship no. SFRH/BD/5207/2001, and by Fundação Calouste Gulbenkian, Research-Grant Process No. 72515. We would also like to thank Luis Matias and an anonymous reviewer, for their detailed and helpful comments, which helped to improve the manuscript.

## Appendix A. Supplementary data

Supplementary data associated with this article can be found, in the online version, at doi:10.1016/j.epsl.2010.01.047.

## References

- Abe, K., 1979. Size of great earthquakes of 1837–1974 inferred from tsunami data. *J. Geophys. Res.* 84, 1561–1568.
- Afilhado, A., Matias, L., Shiobara, H., Hirn, A., Mendes-Victor, L., Shimamura, H., 2008. From unthinned continent to ocean: the deep structure of the West Iberia passive continental margin at 38°N. *Tectonophysics* 458, 9–50.
- Alves, T.M., Moita, C., Cunha, T., Ullnaess, M., Myklebust, R., Monteiro, J.H., Manuppella, G., 2009. Diachronous evolution of Late Jurassic/Cretaceous continental rifting in the northeast Atlantic (west Iberian margin). *Tectonics* 28, TC4003. doi:10.1029/2008TC002337.
- Argus, D.F., Gordon, R.G., DeMets, C., Stein, S., 1989. Closure of the Africa–Eurasia–North America plate motion circuit and tectonics of the Gloria Fault. *J. Geophys. Res. Solid Earth Planets* 24, 5585–5602. doi:10.1016/j.marpetgeo.2007.11.008.
- Arthaud, F., Matte, P., 1977. Late Paleozoic strike-slip faulting in Southern Europe and Northern Africa: result of a right-lateral shear zone between the Appalachians and the Urals. *Geol. Soc. Amer. Bull.* 88, 1305–1320.
- Baptista, M.A., Miranda, P.M.A., Miranda, J.M., Mendes Victor, L., 1998. Constrains on the source of the 1755 Lisbon tsunami inferred from numerical modeling of historical data on the source of the 1755 Lisbon tsunami. *J. Geodyn.* 25, 159–174.
- Baptista, M.A., Miranda, J.M., Chierici, F., Zitellini, N., 2003. New study of the 1755 earthquake source based on multi-channel seismic survey data and tsunami modeling. *Nat. Hazards Earth Syst. Sci.* 3, 333–340.
- Borges, J.F., Fitas, A.J.S., Bezzeghoud, M., Teves-Costa, P., 2001. Seismotectonics of Portugal and its adjacent Atlantic area. *Tectonophysics* 337, 373–387.
- Bufoen, E., Bezzeghoud, M., Udías, A., Pro, C., 2004. Seismic sources on the Iberia–African plate boundary and their tectonic implications. *Pure Appl. Geophys.* 161, 623–646.

- Burov, E., Diament, M., 1996. Isostasy, equivalent elastic thickness, and inelastic rheology of continents and oceans. *Geology* 24, 419–422.
- Burov, E., Poliakov, A., 2001. Erosion and rheology controls on synrift and postrift evolution: verifying old and new ideas using a fully coupled numerical model. *J. Geophys. Res.* 106, 16,461–16,481. doi:10.1029/2001JB000433.
- Calais, E., DeMets, C., Nocquet, J.M., 2003. Evidence for a post-3.16-Ma change in Nubia–Eurasia–North America plate motions? *Earth Planet. Sci. Lett.* 216, 8–92.
- Close, D.I., Watts, A.B., Stagg, H.J.M., 2009. A Marine geophysical study of the Wilkes Land rifted continental margin, Antarctica. *Geophys. J. Int.* 138, 831–850.
- Cunha, T., 2008. Gravity anomalies, flexure, and the thermal and mechanical evolution of the West Iberia Margin and its conjugate of Newfoundland. PhD Thesis, Department of Earth Sciences, Oxford University.
- DeMets, C., Gordon, R.G., Argus, D.F., Stein, S., 1994. Effect of recent revisions to the geomagnetic reversal time scale on estimates of current plate motions. *Geophys. Res. Lett.* 21, 2191–2194.
- Dewey, J.F., Helman, M.L., Turco, E., Hutton, D.H.W., Knot, S.D., 1989. Kinematics of the western Mediterranean. *Spec. Publ. Geol. Soc.* 45, 265–283.
- Diez, S., Gracia, E., Gutscher, M.A., Matias, L., Mulder, T., Terrinha, P., Somoza, L., Zitellini, N., De Alteris, G., Henriot, J.P., Dañobeitia, J., 2005. Bathymetric map of the Gulf of Cadiz, NE Atlantic Ocean: the SWIM multibeam compilation. 250th Anniversary of the 1755 Lisbon Earthquake, Lisbon (Portugal), 1–4 Novembre.
- Fernandes, R.M.S., Ambrosius, B.A.C., Noomen, R., Bastos, L., Wortel, M.J.R., Spakman, W., Govers, R., 2003. The relative motion between Africa and Eurasia as derived from ITRF2000 and GPS data. *Geophys. Res. Lett.* 30 (16), 1828. doi:10.1029/2003GL017089.
- Fukao, Y., 1973. Thrust faulting at a lithospheric plate boundary. The Portugal earthquake of 1969. *Earth Planet. Sci. Lett.* 18, 205–216.
- Gracia, E., Dañobeitia, J., Vergés, J., the Parsifal Team, 2003. Mapping active faults offshore Portugal (360 N–380 N): implications for the seismic hazard assessment along the southwest Iberian margin. *Geology* 31, 83–86.
- Grimison, N.L., Chen, W.P., 1986. The Azores–Gibraltar plate boundary: focal mechanisms, depths of earthquakes and their tectonic implications. *J. Geophys. Res.* 91, 2029–2047.
- Gutscher, M.A., Malod, J.A., Rehault, J.P., Contrucci, I., Klingelhoefer, F., Mendes-Victor, L., Spakman, W., 2002. Evidence for active subduction beneath the Gibraltar. *Geology* 30, 1071–1074.
- Hayward, N., Watts, A.B., Westbrook, G.K., Collier, J., 1999. A seismic reflection and GLORIA study of compressional deformation in the Goringe Bank region, eastern North Atlantic. *Geophys. J. Int.* 138, 831–850.
- Johnston, A.C., 1996. Seismic moment assessment of earthquakes in stable continental regions–III. New Madrid 1811–1812, Charleston 1886 and Lisbon 1755. *Geophys. J. Int.* 126, 314–344.
- Karner, G.D., Watts, A.B., 1983. Gravity anomalies and flexure of the lithosphere at mountain ranges. *J. Geophys. Res.* 8, 10,449–10,477.
- Kooi, H., Chloetingh, S., Burrus, J., 1992. Lithospheric necking and regional isostasy at extensional basins 1. Subsidence and gravity modeling with an application to the Gulf of Lions Margins. *J. Geophys. Res.* 99, 17,553–17,571.
- Maldonado, A., Campillo, A.C., Mauffret, A., Alonso, B., Woodside, J., Campos, J., 1992. Alboran Sea Late Cenozoic tectonic and stratigraphic evolution. *Geo-Mar. Lett.* 12, 179–186.
- Mauffret, A., Mougnot, D., Miles, P.R., Malod, J.A., 1989. Cenozoic deformation and Mesozoic abandoned spreading center in the Tagus Abyssal Plain (west Portugal). Results of a multichannel seismic survey. *Can. J. Earth Sci.* 26, 1101–1123.
- Pinheiro, L.M., Whitmarsh, R.B., Miles, P.R., 1992. The ocean-continent boundary off the western continental margin of Iberia–II. Crustal structure in the Tagus Abyssal Plain. *Geophys. J. Int.* 109, 106–124.
- Pinheiro, L.M., Wilson, R.C.L., Pena dos Reis, R., Whitmarsh, R.B., Ribeiro, A., 1996. In: Whitmarsh, R.B., Sawyer, D.S., Klaus, A., Mason, D.G. (Eds.), *The Western Iberia Margin: a geophysical overview*. Proc. ODP, Sci. Results, 149. Ocean Drilling Program, College Station, TX, pp. 3–19.
- Ribeiro, A., Kullberg, M.C., Kullberg, J.C., Manuppella, G., Phipps, S., 1990. A review of Alpine tectonics in Portugal: foreland detachment in basement and cover rocks. *Tectonophysics* 184, 357–366.
- Ribeiro, A., Cabral, J., Baptista, R., Matias, L., 1996. Stress patterns in Portugal mainland and the adjacent Atlantic region, West Iberia. *Tectonics* 15 (2), 641–659.
- Ribeiro, A., Mendes-Victor, L., Cabral, J., Matias, L., Terrinha, P., 2006. The Lisbon earthquake and the beginning of closure of the Atlantic. *Eur. Rev.* 14, 193–205.
- Rodger, M., Watts, A.B., Greenroyd, C.J., Peirce, C., Hobbs, R.W., 2006. Evidence for unusually thin oceanic crust and strong mantle beneath the Amazon Fan. *Geology* 34, 1081–1084. doi:10.1130/G22966A.1.
- Rosenbaum, G., Lister, G.S., Duboz, C., 2002. Reconstruction of the tectonic evolution of the western Mediterranean since the Oligocene. *J. Virtual Explor.* 8, 107–130.
- Rovere, M., Ranero, C.R., Sartori, R., Torelli, L., Zitellini, N., 2004. Seismic images and magnetic signature of the Late Jurassic to Early Cretaceous Africa–Eurasia plate boundary off SW Iberia. *Geophys. J. Int.* 158 (2), 554–556.
- Sandwell, D.T., Smith, W.H.F., 1997. Marine gravity anomaly from Geosat and ERS-1 satellite altimetry. *J. Geophys. Res.* 102, 10039–10054. doi:10.1029/96JB03223.
- Sartori, R., Torelli, L., Zitellini, N., Peis, D., Lodolo, E., 1994. Eastern segment of the Azores–Gibraltar line (central-eastern Atlantic): an oceanic plate boundary with diffuse compressional deformation. *Geology* 22 (6), 555–558.
- Sella, G.F., Dixon, T.H., Mao, A., 2002. REVEL: a model for recent plate velocities from space geodesy. *J. Geophys. Res.* 107 (B4). doi:10.1029/2000JB000033.
- Solares, J.M.M., Arroyo, A.L., 2004. The great historical 1755 earthquake. Effects and damage in Spain. *J. Seismol.* 8 (2), 275–294.
- Stewart, J., Watts, A.B., Bagguley, J., 2000. Three-dimensional subsidence analysis and gravity modelling of the continental margin offshore Namibia. *Geophys. J. Int.* 141, 724–746. doi:10.1046/j.1365-246x.2000.00124.x.

- Stich, D., Mancilla, F., Pondrelli, S., Morales, J., 2007. Source analysis of the February 12th 2007,  $M_w$  6.0 Horseshoe earthquake: implications for the 1755 Lisbon earthquake. *Geophys. Res. Lett.* 34, L12308. doi:10.1029/2007GL030012.
- Terrinha, P., Pinheiro, L.M., Henriët, J.-P., Matias, L., Ivanov, M.K., Monteiro, J.H., Akhmetzanov, A., Cunha, T., Shaskin, P., Rovere, M., 2003. Tsunamigenic–seismogenic structures, neotectonics, sedimentary processes and slope instability on the southwest Portuguese Margin. *Mar. Geol.* 195, 55–73.
- Vizcaino, A., Gracia, E., Pallas, R., Garcia-Orellana, J., Escutia, C., Casas, D., Willmott, V., Diez, S., Asoli, A., Danobeitia, J., 2006. Sedimentology, physical properties and age of mass transport deposits associated with the Marques de Pombal Fault, Southwest Portuguese Margin. *Norw. J. Geol.* 86 (3), 177–186.
- Watts, A.B., 1988. Gravity anomalies: crustal structure and flexure of the lithosphere at the Baltimore Canyon Trough. *Earth Planet. Sci. Lett.* 89, 221–238.
- Watts, A.B., Burrov, E., 2003. Lithospheric strength and its relationship to the elastic and seismogenic layer thickness. *Earth Planet. Sci. Lett.* 213, 113–131.
- Watts, A.B., Stewart, J., 1998. Gravity anomalies and the segmentation of the continental margin offshore West Africa. *Earth Planet. Sci. Lett.* 156, 239–252.
- Watts, A.B., Talwani, J., 1974. Gravity anomalies seaward of deep-sea trenches and their tectonic implications. *Geophys. J. R. Astron. Soc.* 36, 57–92.
- Wilson, R.C.L., Hiscott, R.N., Willis, M.G., Gradstein, F.M., 1989. The Lusitanian Basin of west-central Portugal: Mesozoic and Tertiary tectonic, stratigraphy, and subsidence history. In: Tankard, A.J., Balkwill, H.R. (Eds.), *Extensional Tectonics and Stratigraphy of the North Atlantic Margins: AAPG Mem.*, 46, pp. 341–361.
- Zitellini, et al., 2001. Source of 1755 Lisbon Earthquake and tsunami investigated. *EOS Trans. Am. Geophys. Union* 82, 282–285.
- Zitellini, N., Rovere, M., Terrinha, P., Chierici, F., Matias, L., the Big-Set Team, 2004. Neogene through Quaternary tectonic reactivation of SW Iberian passive margin. *Pure Appl. Geophys.* 161, 565–587.